Journal of
Materials Chemistry C

ROYAL SOCIETY
OF CHEMISTRY

PAPER

View Article Online
View Journal | View Issue

Cite this: *J. Mater. Chem. C*, 2016, 4, 8459

Received 11th August 2016,
Accepted 18th August 2016

DOI: 10.1039/c6tc03466g

www.rsc.org/MaterialsC

UV irradiation induced reversible graphene band gap behaviors

Zhemi Xu,[a] Zhimin Ao,[b] Dewei Chu*[a] and Sean Li[a]

The nature of zero bandgap has limited the applications of graphene for potential electronic devices, such as p–n junctions and transistors, *etc.* Here we report a simple methodology that can tune the bandgap of graphene by using ultraviolet (UV) irradiation. Most importantly, such a bandgap transition is reversible and can be controlled by the alternative treatment of UV irradiation and dark storage. In addition, density functional theory (DFT) calculations are performed to reveal the underlying mechanism of bandgap behavior in this reversible transition. Both experimental and computational results demonstrate that it is a promising technology for applications of graphene in electronic devices.

1 Introduction

The potential applications of graphene in electronic devices have experienced a rapid expansion over the last decade owing to its unique properties, such as high carrier mobility, excellent optical transparency, and superior mechanical strength, *etc.*[1] However, its potential applications in electronic and photonic devices, such as thin film transistors, *etc.*, have been greatly constrained, due to the zero band-gap and zero local density of states at the Fermi level of graphene.[2,3] Hence, the bandgap opening of graphene has become critical for the applications in various electronic devices.[4] Although several effective techniques, such as patterned hydrogen adsorption,[2] substrate inducing,[5] molecular doping,[6] defect introducing,[7] and quantum dot hybrid,[8] *etc.* have been reported, they either are complicated or may cause damage on the pristine honeycomb structure of graphene, which will degrade the superior properties of the intrinsic graphene.[9]

One of the most effective ways to tune the band gap of graphene is to modify the surface using metal or functional groups, such as epoxide, hydroxyl, hydrogen, fluorine, and water, *etc.*,[9,10] as the band structure of graphene is very sensitive to the lattice symmetry.[11] Hence, such groups on the surface may break the symmetry and result in band-gap opening. It has been widely investigated that the electrical properties of graphene are affected by adsorbed molecules and functional groups. From the theoretical aspect, by doping hydrogen and fluorine, the band gap of graphene on the functionalized hexagonal boron nitride substrate can be increased to 0.079 eV while external electric field can raise the bandgap energy of graphene up to 0.408 eV.[9] From the experimental aspect, a bandgap opening of 0.206 eV has been achieved through adsorbing water molecules on the surface of graphene.[11] Furthermore, a bandgap opening of 0.7 eV has been experimentally realized by surface modification with atomic hydrogen.[12] However, the symmetry broken such methods is hard to avoid owing to the graphene–substrate interaction or patterned adsorption.

Here, we report a simple and effective approach by using UV irradiation to open the bandgap of graphene. It has been experimentally demonstrated that the water molecules can be dissociatively adsorbed on graphene surface by exerting UV treatment on graphene.[13] In this process, the lattice symmetry of the graphene is modified by hydrogen and hydroxyl groups' adsorption from water splitting, resulting in graphene bandgap opening and electric conductivity changing as shown in Fig. 1. Instead of permanent damage, the basic structure of graphene is modified temporarily by the UV irradiation. Particularly the concentration of hydrogen and hydroxyl groups in graphene saturates and the graphene is stabilized after the UV irradiation for one hour. It is reasonable that the bandgap can also eventually

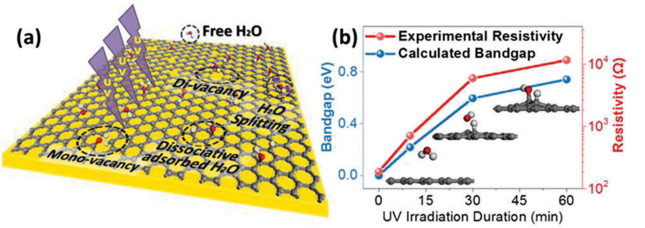

Fig. 1 (a) Schematic diagram of UV irradiation induced H_2O dissociative adsorption on graphene; (b) resistance and bandgap transition of graphene under UV irradiation.

---

[a] *School of Materials Science and Engineering, The University of New South Wales, Sydney, NSW 2052, Australia. E-mail: d.chu@unsw.edu.au*

[b] *Institute of Environmental Health and Pollution Control, School of Environmental Science and Engineering, Guangdong University of Technology, Guangzhou, 510006, China*

be stabilized through prolonging the UV irradiation duration owing to the dissociative adsorption of H_2O molecules.

At the same time, the hydrogen and hydroxyl groups can be desorbed from the graphene surface by placing the irradiated samples in dark environment for a certain time at room temperature, thus restoring the conductivity of graphene. Such an UV irradiation effect on graphene outlines the possibility to realize reversible and controllable graphene bandgap opening process, thus widely expanding its applications in electronics. In addition, first principle study was employed to reveal the mechanism of the band gap opening as well as restoring process of graphene under UV irradiation, so as to fully control the graphene bandgap transition.

2 Methods

2.1 Experimental and characterization details

The as-purchased commercial graphene powder was purchased from Hangzhou Gelanfeng Nanotechnology Co., Ltd and was prepared with oxidation and reduction method. The as-purchased graphene FLG thickness was ~3 nm and the original layer number was ~10. To obtain single layer graphene, original graphene powder in ethanol were ultra-sonicated (John Morris VCX at 750 W) for 1 h, and then were deposited by drop coating on ceramic filter paper for electrical resistance measurement and on glass substrates for ultraviolet-visable (UV-vis) absorbance testing, respectively. To minimize the effects of impurities absorbed on the graphene surface, the as-prepared samples were first dried and dehydrogenated for 2 hours at 100 °C and then illuminated by UV irradiation with the wavelength of 254 nm for 3, 5, 10, 20, 30, 45 and 60 min, respectively. The distance between UV light and graphene samples is 2 cm. In order to minimize the effect of ozone produced by the UV irradiation, the UV chamber was venting during irradiation. A beaker with 150 ml boiled water was put into the UV chamber to increase moisture. Subsequently, the as-irradiated graphene samples were stored in a dark chamber at room temperature for up to 96 h.

Raman spectroscopy with a laser of 514.5 nm wavelength was used for characterizing the graphene thin films. Transmission electron microscopy (TEM) was carried out in a Philips CM200 microscope. A scanning electron microscopy (SEM) system (Nova Nano SEM 450) was used to examine the surface morphology of graphene thin film on filter paper. The resistance of the graphene samples was measured immediately after UV irradiation and dark storage with Autolab 302N electrochemical workstation at room temperature. PerkinElmer UV-visible Spectrometer was used to measure the absorbance of single layer graphene samples with the wavelengths from 200 nm to 800 nm. The glass substrates were used to subtract the background signals.

2.2 Computational methodology

Spin-polarized density functional theory (DFT) calculations were performed in Dmol3 code of Materials Studio package for all geometry optimization and property calculations. The generalized gradient approximation (GGA) function with PW91 correction is employed as the exchange–correlation functional, since it is reported that LDA would underestimate band gaps and would trigger errors of both formation energies and position of electronic transition levels.[14] A double numerical plus polarization (DNP) was employed as the basis set. To consider the effect of van der Waals force, the DFT-D method within the Grimme scheme is used. The convergence tolerance of energy of 10^{-5} Hartree was taken (1 Hartree = 27.21), and the maximal allowed force and displacement were 0.002 Hartree $Å^{-1}$ and 0.005 Å, respectively. To investigate the minimum energy pathway for H_2O molecules dissociative adsorption on graphene surface and defects, linear synchronous transition/quadratic synchronous transit (LST/QST) and nudged elastic band (NBE) tools in Dmol3 code are employed, to find the structure of the transition state and the minimum energy pathway of a reaction. In this simulation, three-dimensional periodic boundary conditions are taken and a vacuum width of 18 Å has applied to all the supercell to minimize the interlayer interaction. The *K*-point is set to 5 × 5, and all atoms are allowed to relax.

3 Results and discussion

3.1 Graphene characterization

Fig. 2(a) compares the 514 nm Raman spectra of graphene thin film before and after UV irradiation. The most strong peaks of pristine graphene Raman spectra agreed well with the previous reports,[13] which are identified as G band at ~1580 cm^{-1} and 2D band at ~2700 cm^{-1}. The 2D band enlargement as inserted shows a typical single layer shape[15] of graphene. D band at ~1350 cm^{-1} is observed in Raman spectra of pristine graphene, but relatively less significant. As shown in Fig. 2(a), after UV-irradiation, the intensity of all the peaks increase significantly, and a new peak at ~3250 cm^{-1} is observed. Such results agreed perfectly with the reported work.[13] Due to the dissociative

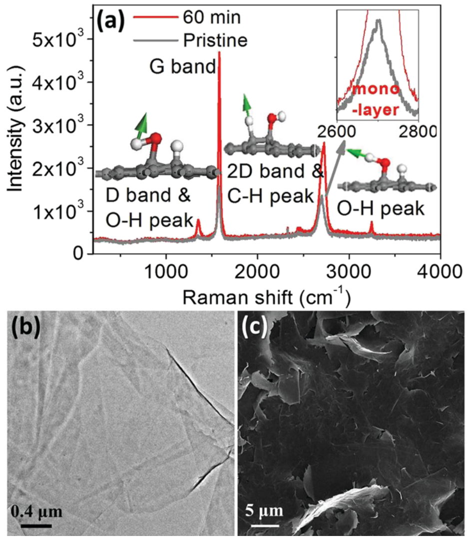

Fig. 2 (a) Raman spectrum of graphene thin film on glass substrates (inset: enlarged 2D band of pristine graphene); (b) TEM of graphene raw solution; (c) SEM of pristine graphene thin film on filter paper.

adsorption of H_2O molecules on the graphene surface under UV irradiation, the formation of C–OH and C–H bonds are facilitated, which caused D band and 2D band peak increases, and a new peak at $\sim$3250 cm^{-1} as marked in Fig. 2(a). Corresponding Raman vibrations of H_2O dissociatively adsorbed graphene were calculated to explain the rise of corresponding Raman peaks. Fig. 2(b) shows a TEM image of a single layer graphene. The SEM image of a typical crumpled and flake-like surface of pristine graphene on filter paper is shown in Fig. 2(c). After UV treatment, the winkle on the surface becomes more obvious.

3.2 Electrical conductivity and optical properties transition under UV irradiation

The resistivity of graphene as a function of UV irradiation time is plotted in Fig. 3(a). It demonstrates that the resistivity of graphene film increases gradually from 185.3 Ω to $\sim$11.5 kΩ under UV irradiation within the first 60 min, and then almost remains as a constant. Current–voltage (*I–V*) curves under voltage sweeping mode, in the sequence of $0 \rightarrow 2 \rightarrow 0 \rightarrow -2 \rightarrow 0$, are detailed in Fig. 3(b). With the increase of UV treatment duration, the response current on graphene sample dropped significantly from $\sim 10^{-2}$ A to almost $\sim 10^{-4}$ A when ± 2 V voltage applied. In Fig. 3(c), the optical properties of graphene thin film on slide glass substrates were measured by UV-vis spectroscopy. The absorption at $\sim$280 nm is consistent with the reported work,[16] which is related to the excitation of π-plasmon of graphite structure. In Fig. 3(c), the absorption peak of pristine graphene at 295 nm gradually blueshifts to 277 nm with UV irradiation time increasing. Such blueshift is considered as electronic conjugation disturbance.[17]

As reported,[13] transition of graphene under UV irradiation is mainly related to the dissociative adsorption of H_2O molecular, and the adsorbed hydrogen and hydroxyl groups may significantly increase the hydrophilicity of graphene as inserted in Fig. 3(a). Thus, it is also reasonable to believe that the adsorbed H and OH groups may disturb the unique graphene structure – π bond and its lattice symmetry, which weakens its electric conduction (Fig. 3(b)), leads to the blueshift in UV-vis spectra (Fig. 3(c)), and may open the band gap.

3.3 Energy band gap and PDOS analysis of UV irradiated graphene

It is known that the band gap is a major factor determining the electrical conductivity. Hence, in order to verify whether UV irradiation can open the band gap of graphene, it is necessary to calculate and compare the band structures and partial density of states (PDOS) of graphene with and without dissociatively adsorbed H_2O at various concentrations. All atomic structures for DFT calculations are presented in Fig. 4. The defect-free graphene and that with adsorbed H and OH group were calculated in various supercell, representing different concentrations of water dissociative adsorption. The calculated structures are periodic supercell, a bigger supercell with one H and OH group representing a lower adsorption concentration. Different positions with H and OH dissociative adsorption on graphene (*ortho*, *meta* and *para* position on a carbon ring) are considered for each structure and the structures with the lowest energy were selected as the final structures of UV irradiated graphene with H and OH as illustrated in Fig. 4 (FS).

The energy band structures (left) and density of states (right) of pristine graphene are shown in Fig. 5(a). Two π bands of graphene join together at the Fermi level at *K* point, while the

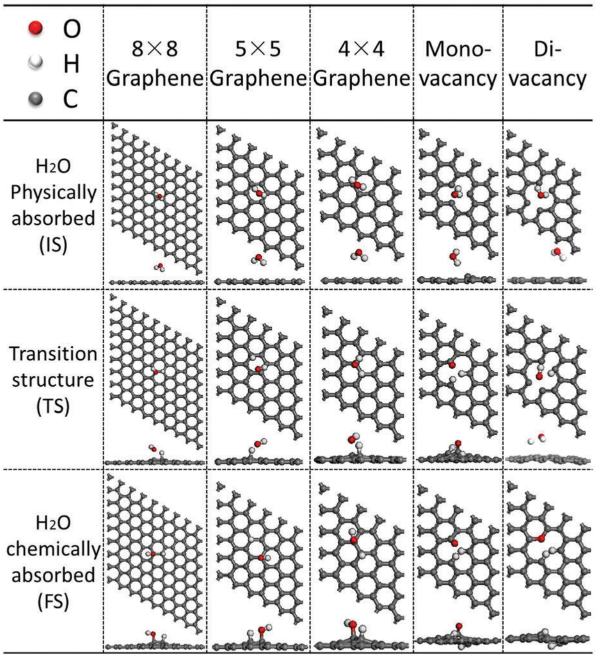

Fig. 4 Atomic structures of graphene before and after one H_2O molecule dissociative adsorption.

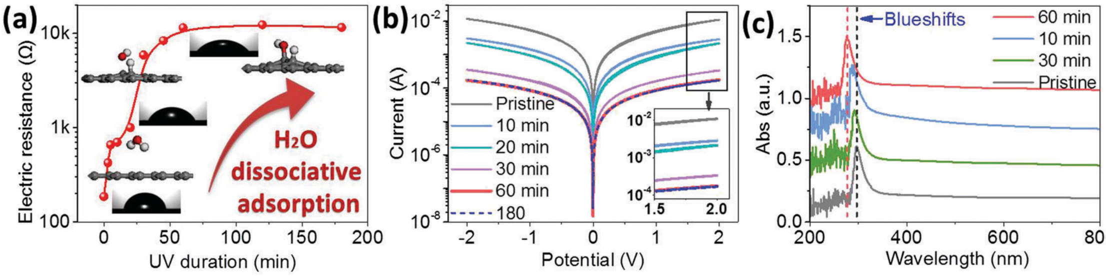

Fig. 3 (a) Electric resistance transition under UV irradiation; (b) IV curves in semi-logarithmic scale; (c) UV-vis absorbance spectrum transition under UV irradiation.

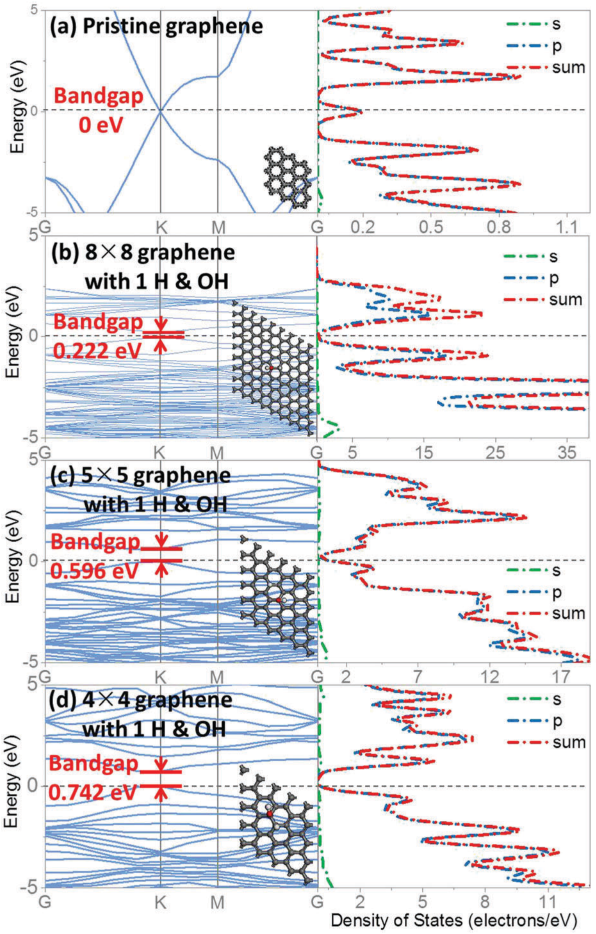

Fig. 5 The computational band structures and PDOS of graphene with different concentration H_2O dissociatively adsorbed.

σ bands are widely separated and a 0.2 electrons per eV peak in its corresponding PDOS is shown in Fig. 5(a, right). This demonstrates the contribution of p orbital, evidencing that the π bands predominate the electrical transport properties of graphene. However, for the graphene with dissociatively adsorbed water molecular at a relative low concentration, in Fig. 5(b), the 8 × 8 supercell band structures show a similar π band character at *K* point but exhibit a direct 0.222 eV band gap between the bonding and antibonding π bands. Accordingly, the PDOS spectra peak contributed by p orbital around Fermi level disappeared. Such a transition was caused by the formation of C–H and C–OH bonds on graphene from water splitting, thus breaks the well dispersed π bands and restricting the electrical transportation.

The higher concentrations of H_2O dissociative adsorption on graphene were calculated in 5 × 5 and 4 × 4 supercell graphene and shown in Fig. 5(c and d). Compared with the 8 × 8 supercell graphene in Fig. 5(b), the band gap energy at *K* point increased to 0.596 eV and 0.742 eV, while the shape of π bands remains. Similarly, the p orbital around Fermi level disappeared in PDOS spectra. The calculated band gap open tendency highly agreed with the decrease of electrical conductivity as shown in Fig. 3(a) and (b) as well as the blueshift of UV-vis absorbance of graphene [Fig. 3(c)]. Specifically, due to the adsorption of H and OH groups, π bands of graphene was disturbed, and graphene band gap was opened at Fermi level. Thus, UV light can act as a switch to open graphene band gap effectively to ∼0.75 eV by H_2O molecules adsorption on its surface, and the band gap can be tuned by concentration of adsorbed H_2O molecules.

3.4 Reaction pathways of H_2O dissociative adsorption on graphene

Although band gap of graphene can be gradually opened by increasing concentration of H and OH groups adsorption, it is necessary to explore the possible concentration H_2O dissociative adsorption on graphene. To confirm whether there is a limitation of adsorption concentration, the reaction pathways of H_2O adsorption on graphene have been calculated and illustrated in Fig. 6. Low to high water adsorption concentrations have been considered, represented by one H_2O molecule dissociative adsorption on 8 × 8, 5 × 5 and 4 × 4 supercell graphene, respectively. All possible reaction pathways are studied with LST/QST and NEB tools in Dmol3 module in Materials Studio software package. It is believed that these methodologies are capable of determining the structures of transition state and the minimum energy pathway for small molecule dissociation and adsorption on graphene.[18] In order to correct the effects of van der Waals interactions and different functional groups in the calculations, DFT-D correction was applied.

As to the reaction pathways shown in Fig. 6, the initial structures (IS), transition structures (TS) and final structures (FS) for each reaction were presented. The top and side views of

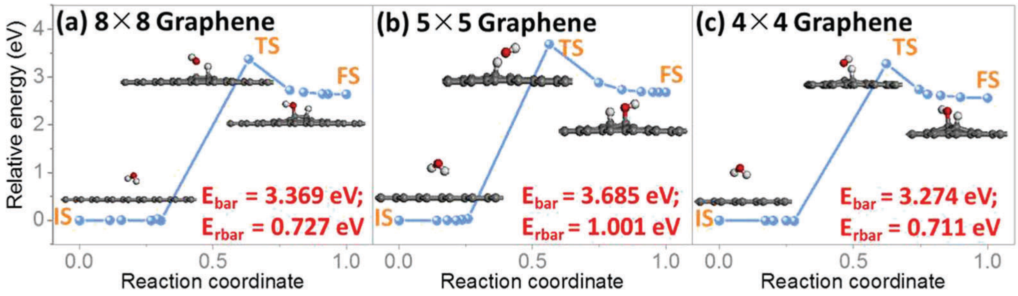

Fig. 6 The reaction path ways for one H_2O molecule dissociatively adsorbed on graphene with different supercell.

each structure can be found in Fig. 4. The initial state is the pristine graphene with a H_2O molecule physically adsorbed over the surface of graphene; the transition state is the state with the highest reaction energies during the reaction, and the final state is the H and OH group chemically adsorbed on graphene surface, which are the same with those shown in Fig. 5. Thus, the reaction energy barrier as $E_{\text{bar}} = E_{\text{TS}} - E_{\text{IS}}$ and the reverse reaction energy barrier is calculated as $E_{\text{rbar}} = E_{\text{FS}} - E_{\text{IS}}$. As shown in Fig. 6, all the reaction barriers of H_2O dissociative adsorption on various graphene supercell are almost the same, which are 3.369 eV, 3.685 eV and 3.274 eV for 8 × 8, 5 × 5, and 4 × 4 supercell system, respectively. For such reaction with an energy barrier around 3.3 eV, UV is sufficient to act as an energy source to facilitate the reaction. Meanwhile, there is no direct link between H_2O dissociative adsorption concentration and the reaction energy barrier, which means H_2O can dissociatively adsorb on graphene surface continuously until saturated, instead of gradually stopping while H_2O concentration increasing. Hence, it is reasonable to believe band gap of graphene can be opened through UV irradiation and theoretically, can reach ∼0.75 eV as calculated.

3.5 Recovery of UV irradiated graphene in dark storage

In Fig. 6, it is noticeable that the reverse energy barriers of H_2O adsorption are relative low, which are 0.727 eV, 1.001 eV and 0.711 eV, respectively. Normally, a reaction with an energy barrier less than 0.75 eV can occur under ambient conditions,[19] *i.e.*, the reaction can occur spontaneously without any extra energy to start. That is to say the H_2O desorption from graphene is possible after UV irradiation. Thus, in order to explore whether the graphene band gap open process is reversible and how long the opened band gap lasts, the recovery tests of UV irradiated graphene has been investigated.

Fig. 7(a) and (b) plot the restored electrical conductivity as a function of the dark storage time, demonstrating a reverse resistance transition of the UV irradiated graphene. With the dark storage, the adsorbed H and OH groups gradually desorbed from the graphene surface. Accordingly, the electrical conductivity of the UV-irradiated graphene films can be substantially restored from 11.5 kΩ to 9.6 kΩ after 24 h, 8.1 kΩ after 48 h, and 4.6 kΩ after 72 h, respectively. The electric resistance remains as a constant after 72 h. Compared with the as-irradiated graphene, the resistance of graphene recovered by 60% after 96 h dark storage. Same reversible transition is observed in graphene hydrophilic properties as inserted in Fig. 7(a). Similarly, in Fig. 7(c), the redshifts in UV-vis spectrum peaks indicate the restore of the electronic conjugation within graphene. After dark storage for 96 h, the H and OH groups on graphene surface desorbed. Accordingly, the graphene structure – π bond and its lattice symmetry recovered. Such a phenomenon demonstrates the transition of graphene electrical properties is reversible. After 1 h UV irradiation, the opened band gap of graphene can last at least 48 h and will recover by ∼60% in 96 h.

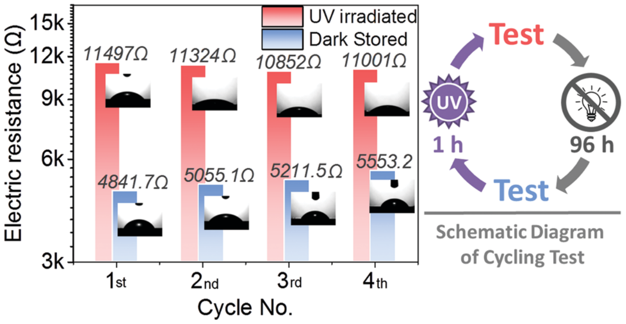

Fig. 8 Reversible graphene conductivity transition in a 4 cycle test by alternative 1 h UV treatment and 96 h dark storage.

For reversible transitions, cycling test is necessary to investigate endurance performance. 4 cycle reversible transition of graphene under and after UV irradiation was studied and shown in Fig. 8. Within every testing cycle, graphene thin film was treated by 1 h UV irradiation (red column) and followed by 96 h dark storage (blue column), and then the next cycle began from 1 h UV irradiation again. As is shown in red columns, the level of graphene electric conductivity remains at 11 kΩ each test after UV irradiation, while the recover level of that increases gradually. Similar tendency is observed in graphene wettability as inserted. Such phenomenon indicates the endurance of graphene band gap open process is reliable through H_2O dissociative adsorption under UV irradiation, while the recovery will be less effective after several irradiation and dark storage cycles.

3.6 Effects of graphene defects on H_2O dissociative adsorption process

In view of the decreased recovery efficiency in cycling test, it is important to consider whether such phenomenon was caused

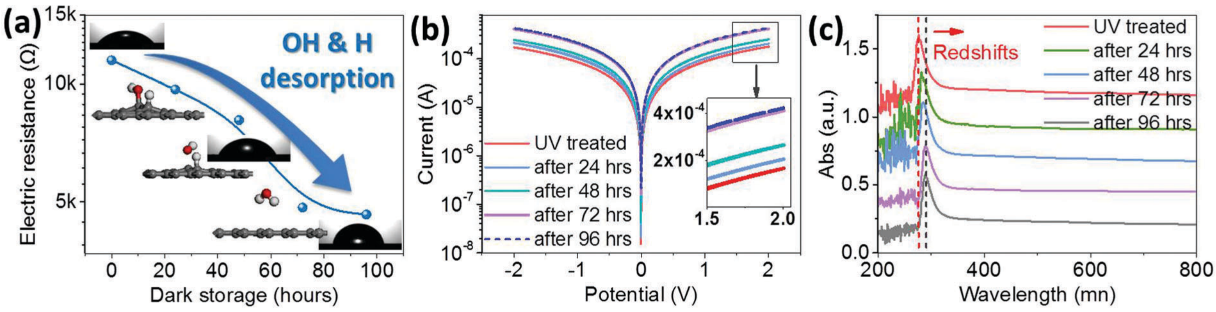

Fig. 7 (a) Electric resistance recovery in dark storage; (b) IV curves in semi-logarithmic scale; (c) UV-vis absorbance spectrum transition in dark storage.

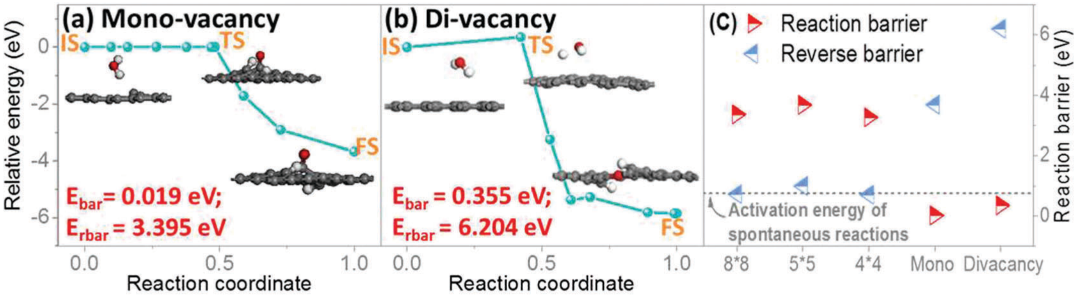

Fig. 9 The reaction path ways for one H_2O molecule dissociative adsorbed on graphene at (a) mono-vacancy and (b) di-vacancy; (c) a comparison of reaction and reverse energy barrier of H_2O dissociative adsorption on pristine and defective graphene.

by the pristine graphene defects and defects that may be induced by UV irradiation. It was reported that one and two carbon atomic vacancies, namely mono-vacancy and di-vacancy, are the most common defects of graphene.[20] In addition, similar with plasma treatment,[21] UV irradiation may induce imperfection and defects to graphene. Thus, to confirm the effects of these defects, 4 × 4 supercell graphene structures with mono-vacancy and di-vacancy were studied. The reaction pathway of one H_2O molecule dissociative adsorption at mono-vacancy and di-vacancy of graphene was shown in Fig. 9(a) and (b). The reaction energy barriers at mono-vacancy and di-vacancy of graphene are very low, 0.019 eV and 0.355 eV, respectively. However, the reverse energy barrier are remarkably high, which are 3.395 eV at mono-vacancy and 6.204 eV for di-vacancy.

A comparison of energy barriers of H_2O dissociative adsorption on pristine and defective graphene is provided in Fig. 9(c). Compared with H_2O dissociative adsorption on pristine graphene, the reaction energy barriers of that on defective graphene are much lower than spontaneous reaction energy barrier(grey line). This means defects, *e.g.*, mono-vacancy and di-vacancy, can facilitate H_2O molecules dissociative adsorption on graphene. However, in the recovering process for the as-UV irradiated graphene, only H and OH groups absorbed on the defect-free graphene can be desorbed in dark environment. Those attached at the mono-vacancy and di-vacancy of graphene are unlikely to be released due to the high reverse reaction energy barriers, thus impeding the restoring process. Hence, due to the pristine and UV induced defects on graphene, it is reasonable that the as-UV irradiated graphene recovered by only 60% after the first time UV irradiation and dark storage cycle (Fig. 7) and recover efficiency gradually decreased after every cycling test (Fig. 8).

3.7 Defective graphene band gap transition under UV irradiation

Since defects on graphene can affect this reversible transition, it is also important to investigate the band gap of such defective graphene so that to better understand its band gap open mechanism under UV irradiation. The band structures together with PDOS of graphene mono-vacancy and di-vacancy are shown in Fig. 10(a-1) and (b-1), and the figures of those after H_2O dissociatively adsorbed are shown in Fig. 10(a-2) and (b-2), respectively. In Fig. 10(a-1), the band gap of graphene mono-vacancy is 0 eV, which suggests that missing only one C atom would not break the symmetry of π bond. However, the dissociatively adsorbed H_2O opens the π band at *K* point around Fermi level significantly to 0.764 eV as shown in Fig. 10(a-2). The disappeared peak at Fermi level in the PDOS indicates the broken π band and band gap open of graphene due to H and O groups. However, the situation of that at di-vacancy is opposite. In Fig. 10(b-1), the band gap of graphene with di-vacancy defects is 0.550 eV, because of the broken π band by two missing C atoms. Conversely, in Fig. 10(b-2), the absorbed H and O atoms at the di-vacancy fills the atom vacancy and

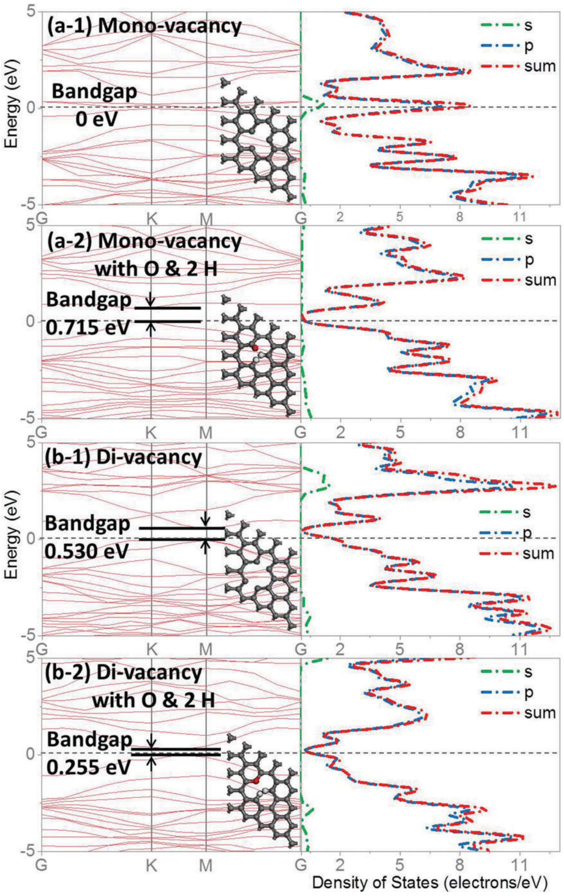

Fig. 10 (a) The band structures and PDOS of graphene mono-vacancy and those with H_2O dissociative adsorbed; (b) the band structures and PDOS of graphene di-vacancy and those with H_2O dissociative adsorbed.

transfers the electrons, thus reducing the band gap energy to 0.222 eV. But overall, owing to the existence of defects, H_2O dissociative adsorption is facilitated, and the desorption is impeded. Hence, defective graphene, such as graphene with mono-vacancy and di-vacancy, makes contributions to the band gap opening under UV irradiation.

4 Conclusion

The combined experimental and calculation results demonstrate that the UV irradiation can act as a switch and result in water dissociative adsorption on graphene, thus inducing a gap in its band structure at Fermi level. The gap induced at Fermi energy depends on the concentration of dissociatively adsorbed H_2O molecule and it is around 0.75 eV for the concentration of one H_2O on 4×4 graphene supercell system, which is sufficient to be utilized for the applications of electronics. Such a transition is reversible and repeatable by alternative UV treatment and dark storage. The opened band gap can last at least 48 and would recover by 60% after 96 h. Furthermore, the presence of defects in graphene would facilitate graphene band gap open and impede the recovery. Such graphene gap opening can be easily achieved. Hence, the results may provide an effective way for the fabrication of graphene based electronic devices, which requires the modification of graphene with different hydrophilicity or band gap.

Acknowledgements

The authors would like to acknowledge the financial support from the Australian Research Council Projects of DP140104373, DP150103006, and FT140100032. ZA acknowledges the financial supports from '100 talents' program of Guangdong University of Technology, '1000 plan' for young professionals program of Chinese Government. Feng Zhang is acknowledged for the assistance in typesetting and proofreading.

References

1 F. Bonaccorso, Z. Sun, T. Hasan and A. Ferrari, *Nat. Photonics*, 2010, **4**, 611–622.

2 R. Balog, B. Jørgensen, L. Nilsson, M. Andersen, E. Rienks, M. Bianchi, M. Fanetti, E. Lægsgaard, A. Baraldi and S. Lizzit, *et al.*, *Nat. Mater.*, 2010, **9**, 315–319.

3 C.-S. Park, Y. Zhao, Y. Shon, I. T. Yoon, C. J. Lee, J. D. Song, H. Lee and E. K. Kim, *J. Mater. Chem. C*, 2015, **3**, 4235–4238.

4 P. Avouris, *Nano Lett.*, 2010, **10**, 4285–4294.

5 S. Zhou, G.-H. Gweon, A. Fedorov, P. First, W. De Heer, D.-H. Lee, F. Guinea, A. C. Neto and A. Lanzara, *Nat. Mater.*, 2007, **6**, 770–775.

6 J. Park, S. B. Jo, Y.-J. Yu, Y. Kim, J. W. Yang, W. H. Lee, H. H. Kim, B. H. Hong, P. Kim and K. Cho, *et al.*, *Adv. Mater.*, 2012, **24**, 407–411.

7 F. Banhart, J. Kotakoski and A. V. Krasheninnikov, *ACS Nano*, 2010, **5**, 26–41.

8 B. Rajbanshi, S. Sarkar and P. Sarkar, *J. Mater. Chem. C*, 2014, **2**, 8967–8975.

9 S. Tang, J. Yu and L. Liu, *Phys. Chem. Chem. Phys.*, 2013, **15**, 5067–5077.

10 Y. Shen, S. Yang, P. Zhou, Q. Sun, P. Wang, L. Wan, J. Li, L. Chen, X. Wang and S. Ding, *et al.*, *Carbon*, 2013, **62**, 157–164.

11 F. Yavari, C. Kritzinger, C. Gaire, L. Song, H. Gulapalli, T. Borca-Tasciuc, P. M. Ajayan and N. Koratkar, *Small*, 2010, **6**, 2535–2538.

12 J. Zhou, M. M. Wu, X. Zhou and Q. Sun, *Appl. Phys. Lett.*, 2009, **95**, 103108.

13 Z. Xu, Z. Ao, D. Chu, A. Younis, C. M. Li and S. Li, *Sci. Rep.*, 2014, **4**, 6450.

14 A. K. Singh, A. Janotti, M. Scheffler and C. G. Van de Walle, *Phys. Rev. Lett.*, 2008, **101**, 055502.

15 A. Ferrari, J. Meyer, V. Scardaci, C. Casiraghi, M. Lazzeri, F. Mauri, S. Piscanec, D. Jiang, K. Novoselov and S. Roth, *et al.*, *Phys. Rev. Lett.*, 2006, **97**, 187401.

16 G. Wang, X. Shen, J. Yao and J. Park, *Carbon*, 2009, **47**, 2049–2053.

17 D. Li, M. B. Mueller, S. Gilje, R. B. Kaner and G. G. Wallace, *Nat. Nanotechnol.*, 2008, **3**, 101–105.

18 Z. Ao and F. Peeters, *J. Phys. Chem. C*, 2010, **114**, 14503–14509.

19 C. Shang and Z.-P. Liu, *J. Am. Chem. Soc.*, 2011, **133**, 9938–9947.

20 A. Hashimoto, K. Suenaga, A. Gloter, K. Urita and S. Iijima, *Nature*, 2004, **430**, 870–873.

21 Y. J. Shin, Y. Wang, H. Huang, G. Kalon, A. T. S. Wee, Z. Shen, C. S. Bhatia and H. Yang, *Langmuir*, 2010, **26**, 3798–3802.